PHILOSOPHICAL TRANSACTIONS OF THE ROYAL SOCIETY A MATHEMATICAL, PHYSICAL & ENGINEERING SCIENCES

Critical jets in surface waves and collapsing cavities

Michael S. Longuet-Higgins and Hasan N. Oguz

Phil. Trans. R. Soc. Lond. A 1997 **355**, 625-639
doi: 10.1098/rsta.1997.0029

Critical jets in surface waves and collapsing cavities

By Michael S. Longuet-Higgins[1] and Hasan N. Oğuz[2]

[1]*Institute for Nonlinear Science, University of California San Diego, La Jolla, CA 92093-0402, USA*

[2]*Department of Mechanical Engineering, The Johns Hopkins University, Baltimore, MD 21218, USA*

In certain types of collapsing cavities, a highly accelerated inward jet can occur. In other cases, starting from slightly different initial conditions, there is no jet but instead a small bubble is pinched off from the main cavity. At critical values of the initial parameters, separating inward jet formation from bubble pinch-off, the local flow has been found to be self-similar; the axial acceleration increases like $(t_1 - t)^{-\alpha}$, where t_1 is a critical value of the time t and α is a positive constant. In this paper we report calculated values of α for three different classes of initial flows, namely (1) a moving sink in an infinite fluid, (2) a bubble collapsing near a plane wall and (3) a slightly deformed bubble in an infinite fluid, with gravity. These flows are all axisymmetric. The two-dimensional jets arising from the impact of surface waves on a plane wall are also discussed and modelled.

1. Introduction

A vertical jet of water is commonly thrown upwards by the collapse of the cavity in a bubble bursting at the sea surface (Blanchard & Woodcock 1980) and sometimes by the collapse of cavities caused by falling drops of rain (Oğuz & Prosperetti 1990). On a larger scale, a controlled upward jet can be produced by the collapse of the bowl in an axisymmetric standing wave, excited subharmonically (see Longuet-Higgins 1983). Thus in a laboratory experiment with a circular cylinder of radius 8.2 cm, upward velocities exceeding 8 m s^{-1} were measured, with accelerations exceeding $15g$.

Similar jets are often observed when a two-dimensional wave approaches a vertical sea-wall, or a ship's hull. Whereas at low wave amplitudes the free surface remains horizontal and the wave is reflected smoothly, and at high wave amplitudes the surface overturns and traps a volume of air, at some intermediate or critical wave amplitude a jet of water can be thrown violently upwards. In the numerical experiments of Cooker & Peregrine (1991), for example, the upwards acceleration of the jet sometimes exceeded $1850g$.

A similar phenomenon is found in collapsing underwater cavities. It is well known that during the axisymmetric collapse of a bubble or cavity near a solid or a free surface, a strong inward jet usually occurs (Plesset & Chapman 1971). There are, however, some cases, as we shall show, where instead of the smooth formation of a jet, the free surface pinches off a small subsidiary cavity. If the initial flow conditions are allowed to vary continuously, there is a critical value of the parameter at which

Phil. Trans. R. Soc. Lond. A (1997) **355**, 625–639
Printed in Great Britain

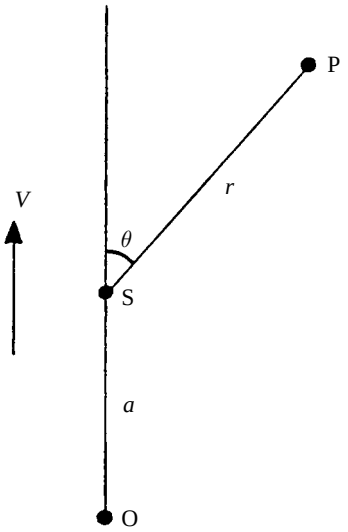

Figure 1. Coordinates (r, θ) for a moving sink S.

bubble 'pinch-off' first occurs. A particular example, when the initial flow is described by a moving point-sink within the cavity, has been analysed by Longuet-Higgins & Oğuz (1995). The initial flows were described by two independent parameters C and D (see § 3). Some attention was paid to the typical case $D = 1$, which became critical when $C \simeq 0.4$. Close to the critical value of C the form of the jet and the corresponding flow were examined and found to be closely self-similar, with the local scale of the jet being proportional to $(t_1 - t)^\beta (\beta \simeq 0.575)$. Thus the particle velocities and accelerations varied as $(t_1 - t)^{\beta-1}$ and $(t_1 - t)^{\beta-2}$, respectively, t_1 being the critical time t. Hence the velocities and accelerations became indefinitely large as $t \to t_1$ (the fluid was assumed incompressible).

In the example just given the flow was unbounded and there was no external pressure field applied at infinity. Moreover, only the case $D = 1$ was considered. In the present paper we shall extend these results in three ways: first, by considering other moving-sink flows, with $D \neq 1$; second by considering the collapse of a slightly asymmetric bubble under gravity, and with a constant applied pressure at infinity; third by considering an asymmetric bubble situated close to a solid wall, with no gravity. These cases are treated in § 2, 3 and 4, respectively. In each case we find critical values of the parameter, separating jet formation and bubble pinch-off, with corresponding velocity fields that are locally self-similar, and we determine the corresponding values of the exponent β. The results are summarized in § 5.

Finally in § 6 we analyse the analogous phenomenon in two-dimensional surface waves. The critical jet, or 'flip through', of Cooker & Peregrine (1990) is taken as an example.

2. Collapse of axisymmetric cavities: the 'moving sink' solution

In this section we generalize the results of Longuet-Higgins & Oğuz (1995) (referred to as LHO). In that paper the starting values for numerical time-stepping were determined by writing down an exact solution for potential flow and identifying the initial free surface with an instantaneous isobar of the solution. The initial flow was

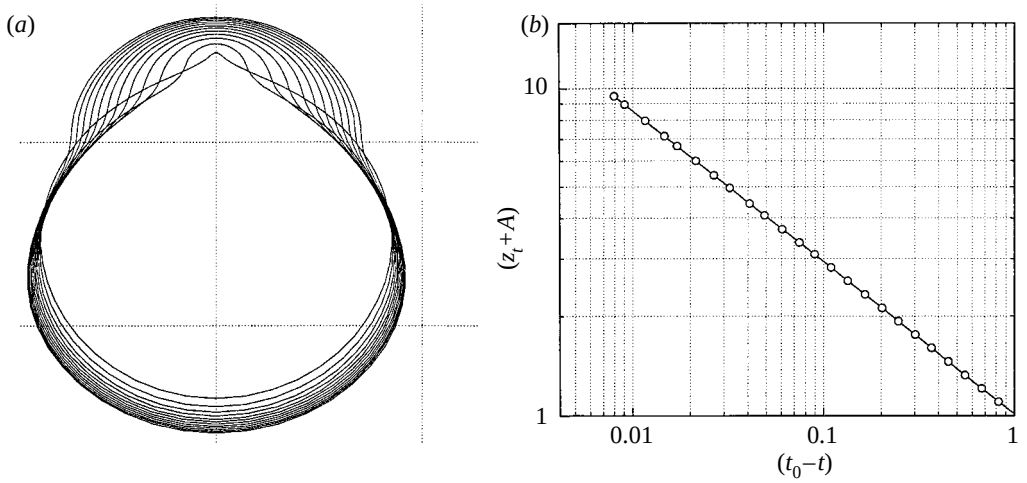

Figure 2. A moving-sink flow. Critical case when $D = 0.8$ and so $C = 0.43$: (a) profiles of the bubble surface; (b) the axial velocity z_t as a function of time.

due to a sink of strength $S(t)$ at the moving point S, situated a distance a from the fixed point O (see figure 1). Thus the initial velocity potential ϕ was given by

$$\phi = \frac{S}{r}, \tag{2.1}$$

where $r(t)$ and $\theta(t)$ are polar coordinates relative to S. The velocity V of the sink is chosen as that

$$V = \frac{S}{a^2}. \tag{2.2}$$

Hence in a frame of reference moving with the sink, the particle velocity at O is initially zero. From Bernoulli's equation one finds the contours of constant pressure $p = p_0$ to be given by

$$\frac{a^4}{r^4} + 2\frac{a^2}{r^2}\cos\theta + D\frac{a}{r} = C, \tag{2.3}$$

where

$$C = -\frac{2(p - p_\infty)}{V^2} \quad \text{and} \quad D = \frac{2\dot{S}}{aV^2}, \tag{2.4}$$

p_∞ being the pressure at infinity, assumed constant, and $\dot{S} = \mathrm{d}S/\mathrm{d}t$. In the typical case $D = 1$, the pressure contours ($C = \text{const.}$) are closed curves (in an axial plane) surrounding the sink S; see LHO, figure 2b. The pressure gradient near the origin is initially very high with a pressure maximum on the axis of symmetry, just below the free surface.

On integrating forwards in time ($t > 0$) one finds typically a strong initial acceleration, producing an inward jet along the axis. On working *backwards* in time (or equivalently reversing the initial flow) one finds surprisingly that the jet moves round to the opposite, or north, pole of the cavity (see LHO, figure 7), provided C exceeds the critical value $C_{\mathrm{crit}} = 0.4$. When on the other hand $C < C_{\mathrm{crit}}$ a jet is not formed but a 'bubble of air' is pinched off. The difference in behaviour is seen clearly by comparing the case $C = 0.45$ (LHO, figure 9a) with the case $C = 0.35$ (LHO, figure 9b).

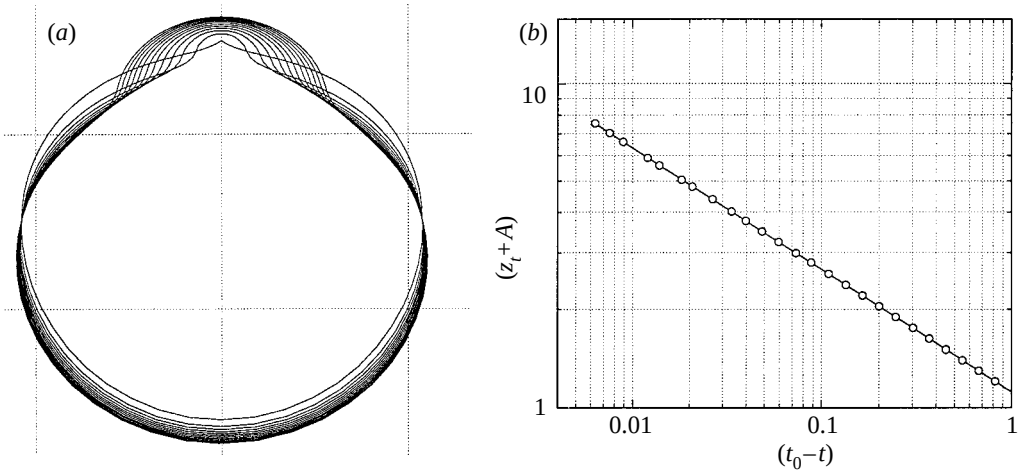

Figure 3. A moving-sink flow. Critical case when $D = 1.4$ and so $C = 0.31$: (a) profiles of the bubble surface; (b) the axial velocity z_t as a function of time.

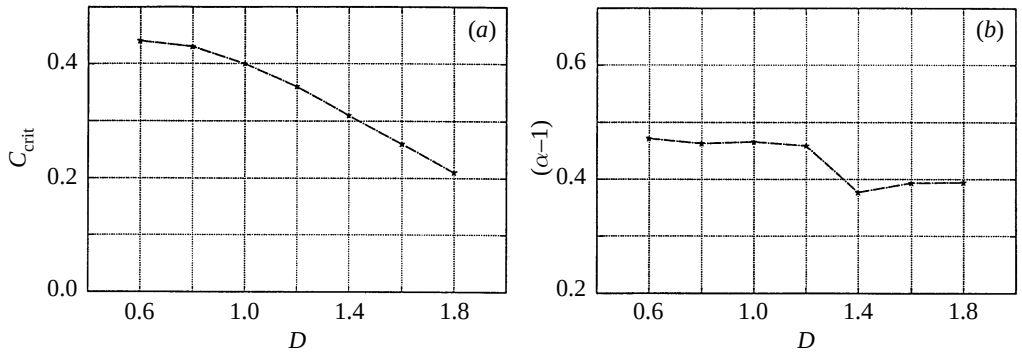

Figure 4. Summary of results for the moving sink: (a) the critical value of C as a function of D; (b) the exponent α as a function of D.

In the critical case $C = 0.40$, the self-similarity of the flow near the critical instant and in the neighbourhood of the 'north pole' is shown in LHO, figures 10–13. We have now carried out similar computations at other values of the parameter D in the range $0.6 \leqslant D \leqslant 1.8$. For each value of D there was a corresponding critical value C_{crit} of C separating jet formation from bubble pinch-off. Examples of the sequence of bubble profiles near the critical time $t = t_1$ are shown in figures 2a and 3a in the typical cases $D = 0.8$ and $D = 1.4$, respectively. In figures 2b and 3b are shown the velocity of a particle on the axis of symmetry, plotted against $(t_1 - t)$ on a logarithmic scale, and showing the power-law behaviour of z_t. The corresponding exponent

$$\alpha - 1 = 1 - \beta \tag{2.5}$$

is plotted in figure 4b, as a function of D. In contrast to the behaviour of C_{crit}, which varies smoothly with D (see figure 4a) we see that α remains almost constant over the range $0.6 \leqslant D \leqslant 1.2$, but then undergoes a transition to somewhat lower values. The reason for this transition is not well understood but will be investigated by comparison with other physical situations.

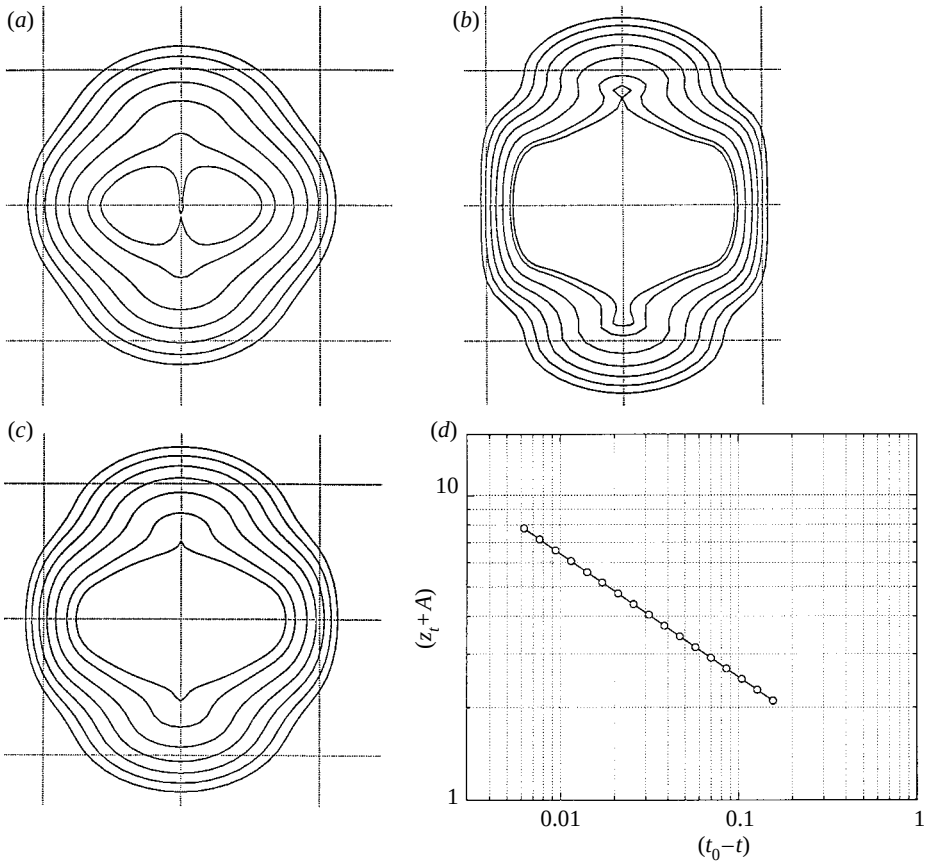

Figure 5. Bubble collapse under gravity. Surface profiles when $D = 0.01$: (*a*) $C = 0.10$; (*b*) $C = 0.30$; (*c*) $C = 0.16$; (*d*) the axial velocity z_t in case (*c*).

3. Bubble collapse under gravity

In this next example we consider the collapse of an almost spherical bubble situated at a depth H below a free surface where the ambient pressure is $p_{\rm atm}$. The maximum diameter of the bubble is assumed small compared to H. The initial shape of the bubble is given in polar coordinates $(r, 0)$ by

$$\zeta/a = 1 + C\mathrm{e}^{-5(\theta-\pi/2)^2}, \tag{3.1}$$

C being a dimensionless constant which controls the up–down asymmetry of the bubble. The initial velocity is assumed to be zero.

If z is a vertical coordinate directed upwards from the centre of the bubble, then the pressure at infinity in the plane $z = 0$ given by

$$p_0 = p_{\rm atm} + \rho g H, \tag{3.2}$$

where ρ is the water density and g is the gravity. Bernoulli's equation may then be written as

$$\frac{D\phi}{Dt} - \frac{1}{2}(\nabla\phi)^2 + \frac{p}{\rho} + gz = \frac{p_0}{\rho}, \tag{3.3}$$

ϕ being the velocity potential. Hence on the surface of the bubble where the pressure

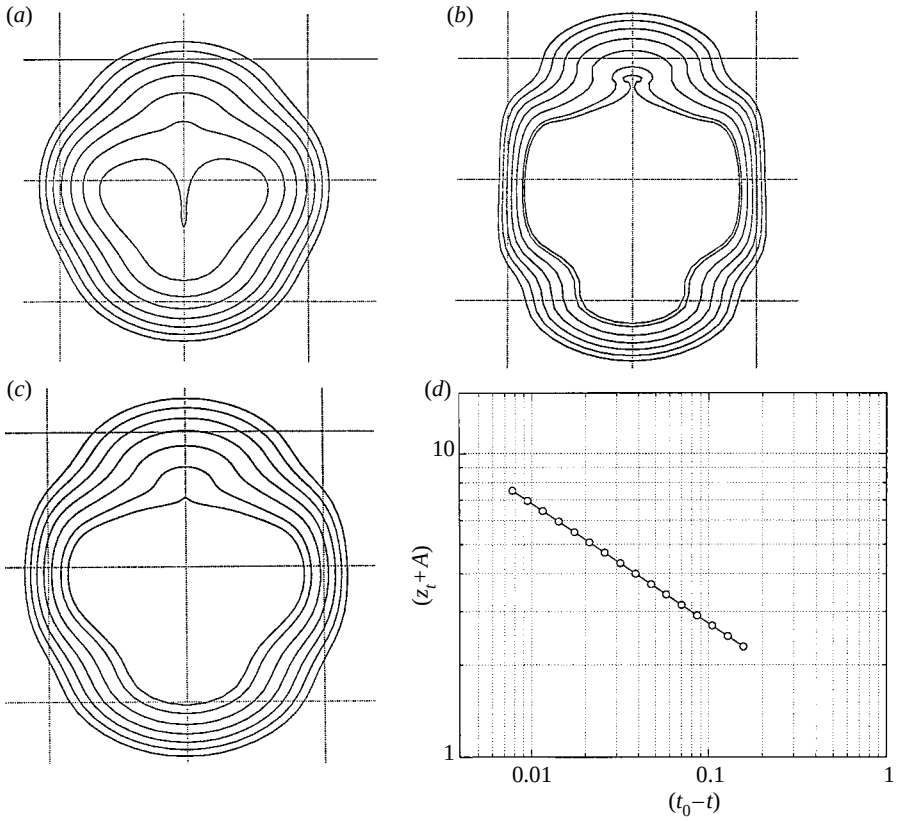

Figure 6. Bubble collapse under gravity. Surface profiles when $D = 1.0$: (*a*) $C = 0.10$; (*b*) $C = 0.30$; (*c*) $C = 0.30$; (*d*) the axial velocity z_t in case (*c*).

p_B is assumed constant we have

$$\frac{D\phi}{Dt} = \frac{1}{2}(\nabla\phi)^2 + \frac{p_0 - p_B}{\rho} + gz. \tag{3.4}$$

It is convenient to choose units so that $\rho = 1$ and $(p_0 - p_B) = 1$, and to write equation (3.4) in the form

$$\frac{D\phi}{Dt} = \frac{1}{2}(\nabla\phi)^2 + 1 + \frac{\rho g z}{p_{atm}} D, \tag{3.5}$$

where

$$D = \frac{p_{atm}}{p_0 - p_B} \tag{3.6}$$

is a dimensionless parameter which controls the effect of gravity on the motion. Note that when $z = a = 50$ cm the dimensionless combination $(\rho g z/p_{atm})$ equals 0.0484.

Figures 5*a*, *b* show the collapse of the bubble when $D = 0.01$ and so the effect of gravity is relatively small. In figure 5*a*, when $C = 0.10$, two inward jets are seen, one upwards and one downwards. In figure 5*b*, when $C = 0.3$, two cavities are formed instead. The critical value of C is 0.16; see figure 5*c*. From figure 5*d* we again see self-similar behaviour with $\alpha = -0.4065$.

On increasing D to 1.0 (see figure 6) so that gravity is relatively more important, we see that when $C = 0.10$ (figure 6*a*) only one jet is formed, and when $C = 0.30$

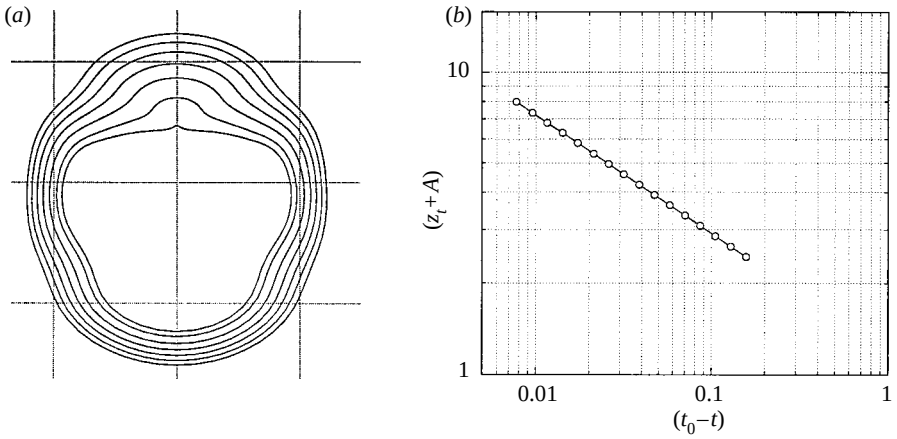

Figure 7. Bubble collapse under gravity ($D = 2.0$). The critical case when $C = 0.16$: (a) Surface profiles; (b) z_t as a function of time.

(figure 6b) there is only one cavity. In the critical case $C = 0.16$ (figure 6c). The behaviour is self-similar as before, but with $\alpha = -0.396$.

When $D = 2.0$ (figure 7) the asymmetry is even more pronounced. Figure 7a shows the surface profile in the critical case $C = 0.16$, and figure 7b the behaviour of z_t. The value of α is very little changed, though it will be noticed that the limiting profile has opened up markedly with the angle between the local asymptotes increased to near 180°.

4. Bubble collapse near a wall

Third we suppose the centre of the bubble to be at a finite distance h from a plane wall. The initial configuration of the bubble surface is given by equation (3.2) as before, but gravity is now neglected. The fluid is initially at rest. We have, then, the dimensionless parameter

$$D = h/a, \tag{4.1}$$

defining the relative distance of the bubble from the wall, and the constant C in equation (4.2) defining the bubble shape.

Figures 8a, b show the development of the profile when $D = 1.1$ and when $C = 0.10$ (jet formation) and when $C = 0.30$ (cavity formation), respectively. The critical value $C = 0.18$ is shown in figure 8c. In this physical situation, critical behaviour was found only at values of D slightly greater than 1 ($D = 1.05$ and $D = 1.10$), that is to say when the bubble was quite close to the wall.

5. Discussion

From the previous examples it is clear that locally self-similar behaviour in the critical flow dividing jet formation from the bubble pinch-off is not peculiar to the moving-sink cavity, but occurs in other situations as well.

However, it is also clear that the exponent α defining the local asymptotic behaviour of the cavity in the critical case is not an absolute constant. We shall now describe a theoretical model which suggests an appropriate value of α for one impor-

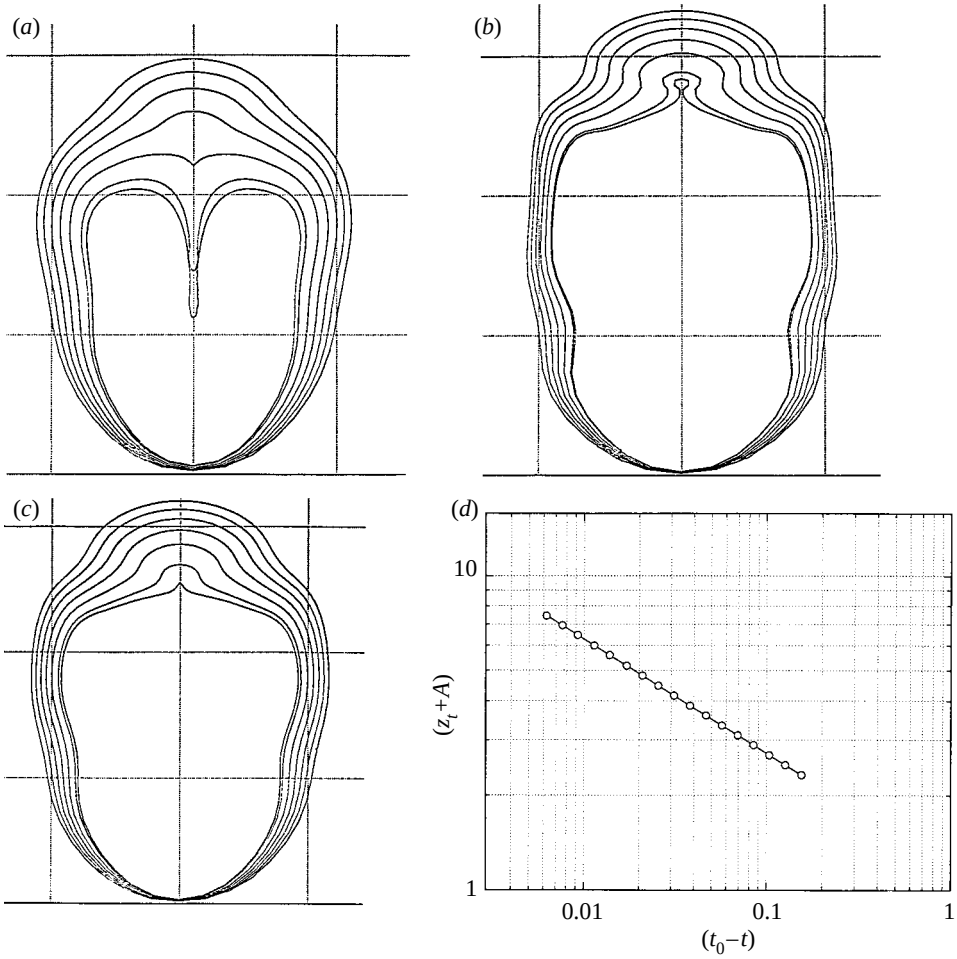

Figure 8. Bubble collapse near a wall. Surface profiles when $D = 1.1$: (*a*) $C = 0.10$; (*b*) $C = 0.30$; (*c*) $C = 0.18$; (*d*) the axial velocity z_t in case (*c*).

tant limiting case. Consider the velocity potential

$$\phi = Ar^{\nu} P_{\nu}(\cos\theta), \tag{5.1}$$

where (r, θ) are fixed polar coordinates, with the axis $\theta = 0$ directed vertically upwards and A is some function of the time t only. P_{ν} denotes the Legendre function of degree ν, non-integral in general. From Bernoulli's equation we find

$$-p/\rho = \dot{A}r^{\nu} P_{\nu}(\mu) + \tfrac{1}{2}A^2 r^{2\nu-2}\Phi(\mu) + f(t), \tag{5.2}$$

where we have set $\mu = \cos\theta$ and

$$\Phi = (\nu P_{\nu})^2 + (1-\mu^2)P_{\nu}'^2, \tag{5.3}$$

with a prime denoting $\mathrm{d}/\mathrm{d}\mu$. A dot denotes differentiation with respect to t. From (5.1) and (5.2) we can write down the material time-derivative Dp/Dt, which after some simplification becomes

$$-\frac{1}{\rho}\frac{Dp}{Dt} = \ddot{A}r^{\nu} P_{\nu} + 2A\dot{A}r^{2\nu-2}\Phi + \dot{f} + A^3 r^{3\nu-4}[\nu(\nu-1)P_{\nu}\Phi + (1-\mu^2)P_{\nu}'\Phi']. \tag{5.4}$$

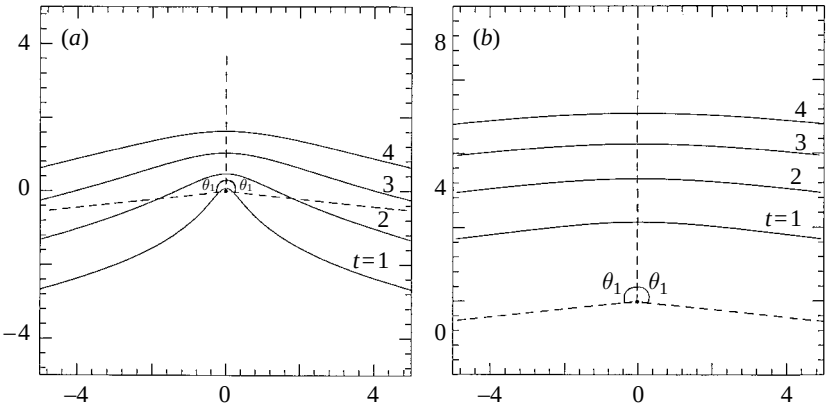

Figure 9. Surface profiles given by equation (5.12) when $\nu = 0.9$: (*a*) $C = 8.0$; (*b*) $C = 0.2$.

Both expressions (5.2) and (5.4) are to vanish on the free surface. We shall discuss the behaviour of these equations in the case when $\nu(\nu-1)$ is small, and in particular when ν is close to one.

Now from the expansion

$$P_\nu = 1 + \frac{\nu(\nu+1)}{1.1}\left(\frac{\mu-1}{2}\right) + \frac{\nu(\nu-1)}{1.2}\frac{(\nu+1)(\nu+2)}{1.2}\left(\frac{\mu-1}{2}\right)^2 + \cdots, \tag{5.5}$$

we see that ν is a factor of $P'_\nu(\mu)$. Similarly it may be shown (see Appendix A) that $(\nu-1)$ is a factor of $\Phi'(\mu)$. Hence when $\nu(\nu-1)$ is small, the coefficient of $r^{3\nu-4}$ in equation (5.4) is in general small. Neglecting this term in comparison to the first two terms in (5.4) we then have two expressions, (5.2) and (5.4) each with only three terms, whose vanishing represents the same surface. Hence the coefficients of corresponding terms are in proportion, that is to say

$$\frac{\ddot{A}}{\dot{A}} = \frac{4A\dot{A}}{A^2} = \frac{\dot{f}}{f}. \tag{5.6}$$

Hence

$$\dot{A} \propto A^4, \tag{5.7}$$

and so

$$t \propto \int \frac{\mathrm{d}A}{A^4} \propto \frac{1}{A^3}. \tag{5.8}$$

Thus

$$A = A_0 t^{-1/3}, \quad f = f_0 t^{-4/3}, \tag{5.9}$$

where A_0 and f_0 are constants and the velocity potential is given by

$$\phi = A_0 t^{-1/3} r^\nu P_\nu(\cos\theta). \tag{5.10}$$

The free surface, from (5.2) is approximately given by

$$-\tfrac{1}{3}A_0 r^\nu P_\nu + \tfrac{1}{2}A_0^2 t^{2/3} r^{2\nu-2}\Phi + f_0 = 0. \tag{5.11}$$

Choosing units so that $A_0 = 2$ and setting $f_0 = -(\frac{2}{3})C$, where C is positive, we obtain

$$r^\nu P_\nu - 3t^{2/3} r^{2\nu-2}\Phi + C = 0. \tag{5.12}$$

Table 1. *Zeros of* $P_\nu(\cos\theta)$

ν	μ_1	θ_1
1.00	0.0000	90.00^o
0.95	−0.0515	92.96^o
0.90	−0.1063	96.10^o
0.85	−0.1644	99.46^o
0.80	−0.2258	103.05^o
0.75	−0.2904	106.88^o

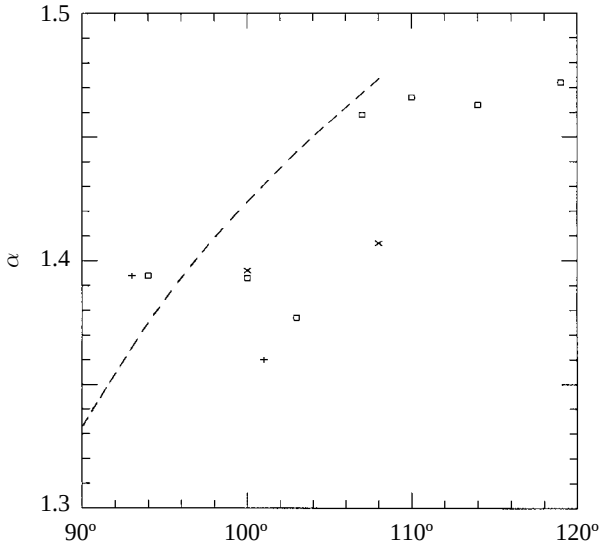

Figure 10. The exponent $\alpha = 2 - \beta$ plotted against the asymptotic angle θ_c for differential physical situations: square plots, moving sink; ×, collapse under gravity; +, collapse near a wall. The broken curve represents the theoretical exponent $[2 - \frac{2}{3}(2-\nu)^{-1}]$ plotted against the first zero θ_1 of $P_\nu(\cos\theta)$.

This can also be written

$$P_\nu = \frac{3t^{(2/3)}\Phi}{r^{2-\nu}} - \frac{C}{r^\nu}. \tag{5.13}$$

Since ν is near unity, the free surface goes to infinity ($r \to \infty$) in a direction $\theta = \theta_1$ where θ_1 is the first zero of $P_\nu(\cos\theta)$:

$$P_\nu(\cos\theta_1) = 0. \tag{5.14}$$

If $\nu < 1$ the surface also crosses the line $\theta = \theta_1$ at a finite value of r (see figure 9). However, the distance of the surface from $\theta = \theta_1$ increases without limit as $r \to \infty$.

Suppose that the constant C, which is at our disposal, is small compared to one. Then provided that neither r nor $P_\nu(\cos\theta)$ is small we have from equation (5.12)

$$r^{2-\nu} \sim (3\Phi/P_\nu)t^{(2/3)}. \tag{5.15}$$

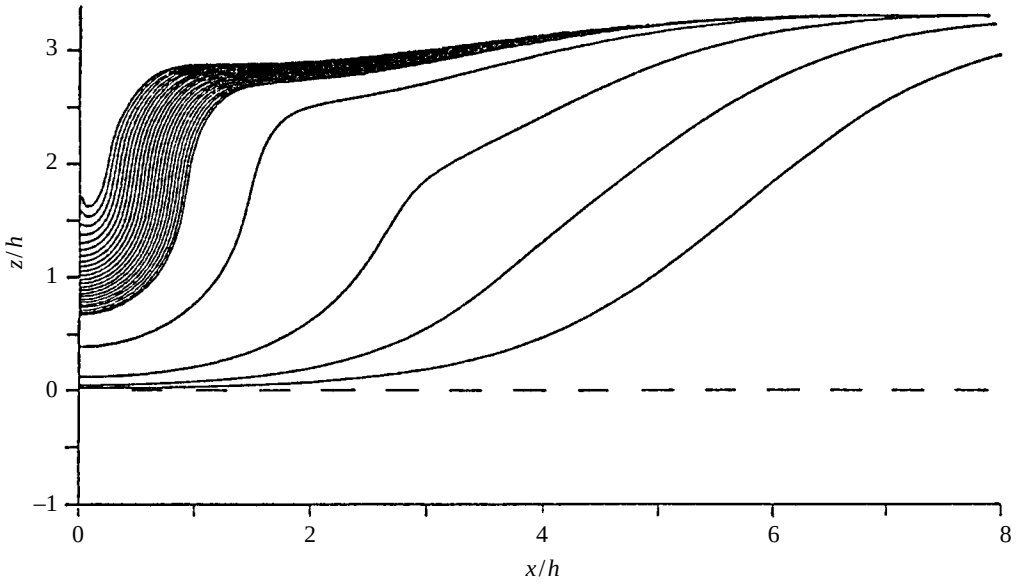

Figure 11. Successive profiles of a shallow-water wave approaching a wall. (after Cooker & Peregrine 1990).

In other words over a certain range of r and θ we have $r \propto t^{\beta}$, where

$$\beta = \frac{2}{3(2-\nu)}. \tag{5.16}$$

In particular for a particle on the axis, where

$$\theta = 0, \quad \mu = 1, \quad P_\nu = 1, \quad \Phi = \nu^2, \tag{5.17}$$

the factor $(3\Phi/P_\nu)$ equals $3\nu^2$ simply. This power-law behaviour breaks down when θ approaches θ_1, and also for very small values of t, depending on the magnitude of C.

Some zeros of P_ν are given in table 1, from which it will be seen that ν is a decreasing function of θ_1. So from equation (5.16) we expect β to decrease and $\alpha = 2 - \beta$ to increase with θ_1. It is interesting to plot the experimental values of α found in §§ 2–4, against the angle θ_c made by the 'asymptotes' with the vertical axis. This is done in figure 10. In the same figure is shown the curve corresponding to the first zero θ_1 of $P_\nu(\cos\theta)$, as derived from the series (5.5). The trend is similar to that page of the plotted points.

On the other hand, as can be seen from figure 9*b*, at small values of C the theoretical surface profiles, though qualitatively similar to the experimental profiles, do not closely match them. We must conclude that the simple potential function (5.1) provides only a first approximation.

6. Critical jets in surface waves

We can give a similar interpretation to the two-dimensional jets in surface waves found by Cooker & Peregrine (1991) which were mentioned in the introduction. Figure 11, from Cooker & Peregrine (1990), shows a computed sequence of surface

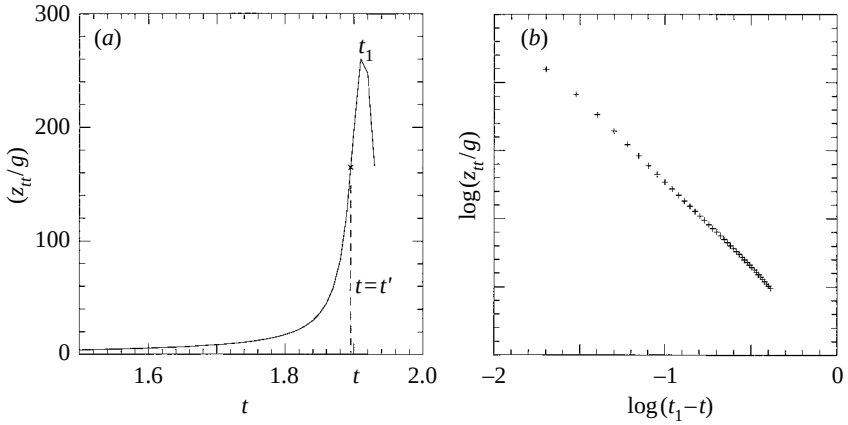

Figure 12. The surface acceleration z_{tt} at $x = 0$, as a function of the time: (a) linear scale; (b) logarithmic scale ($t < t'$).

profiles for a steep surface wave in shallow water meeting a vertical wall at $x = 0$. They are at equal time increments $\Delta t = 0.01(h/g)^{1/2}$, where h is the undisturbed depth of water.

From this data we may estimate the velocity z_t and acceleration z_{tt} of a surface particle at the wall as a function of the time t. The acceleration is shown in figure 12a from which it will be seen that there is a sharp maximum at about $t_1 = 1.91(h/g)^{1/2}$, followed by a rapid fall off. This phase of the motion was called by Cooker & Peregrine the 'flip-through'. At slightly different values of the initial parameters, an air pocket was trapped. Hence the flow in figure 11 can be considered as close to a critical case separating air entrapment from jet formation. In contrast to the numerical cases studied in §§ 2–4 we are here slightly on the jet side of the critical flow.

When plotted on a logarithmic scale against $\ln(t_1 - t)$ the values of the acceleration to the left of the point of inflexion in figure 12a appear as in figure 12b. The plot is very nearly a straight line, corresponding to the power-law

$$z_{tt}/g \propto (t_1 - t)^{-1.22}. \tag{6.1}$$

Consider now the velocity potential

$$\phi = Ar^{\nu} \cos \nu\theta, \tag{6.2}$$

where r and θ are polar coordinates in two dimensions ($\theta = 0$ vertically downwards) and A is some function of the time t only. From Bernoulli's equation we have for the pressure p

$$-p/\rho = \dot{A}r^{\nu} \cos \nu\theta + \tfrac{1}{2}\nu^2 A^2 r^{2\nu-2} + f(t), \tag{6.3}$$

gravity being neglected. The time-derivative of p following a particle is found to be given by

$$-\frac{1}{\rho}\frac{Dp}{Dt} = 2\nu^2 A\dot{A}r^{2\nu-2} + [\ddot{A}r^{\nu} + \nu^3(\nu - 1)A^3 r^{3\nu-4}] \cos \nu\theta + \dot{f}. \tag{6.4}$$

Both p and Dp/Dt are to vanish on the free surface.

If ν is close but not equal to one, then the second term in the coefficient of $\cos \nu\theta$ in (6.4) becomes negligible compared to the first. As in § 5 it follows that $A = A_0 t^{-1/3}$ and $f = f_0 t^{-4/3}$. On choosing $A_0 = 2$ and $f_0 = -\frac{2}{3}C$ we find for the equation of the

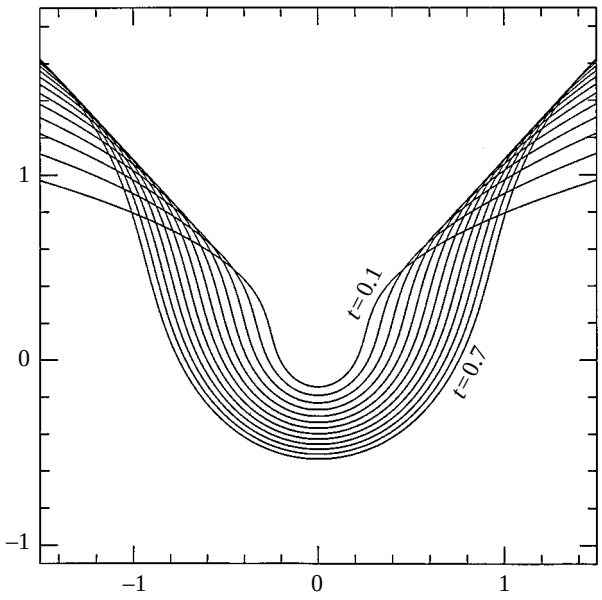

Figure 13. Profiles of the free surface given by equation (6.14) when $\nu = 0.95$, $C = 3.24$ and $t = 0.7(-0.05)0.1$.

free surface

$$r^{\nu} \cos \nu\theta - 3\nu^2 t^{2/3} r^{2\nu-2} + C = 0. \tag{6.5}$$

This may be compared with equation (5.12), in which P_ν is replaced by $\cos \nu\theta$ and Φ is replaced by ν^2, a constant.

The 'asymptotes' of the free surface occur when $r \to \infty$ and $\theta \to \theta_1$, where

$$\theta_1 = \pi/2\nu. \tag{6.6}$$

We see that when C is small and θ is not near θ_1, then $r \propto t^\beta$ as before, β being given by equation (5.18).

As a confirmation of our approximation we note that in equation (6.4) the ratio of the term neglected to that retained is

$$\nu^3(\nu - 1) r^{2\nu-4} A^3 / \ddot{A} \sim (\nu - 1) r^{-2} t^{4/3}, \tag{6.7}$$

which becomes increasingly small as $t \to 0$.

The forms of the free surface, though qualitatively similar to those in figure 9, are not close to them when C is small. However, it may be worth remarking that if the condition on f is relaxed we may have

$$f = -\tfrac{2}{3} C t^{\sigma} \quad \text{and} \quad r = R t^{\beta}, \tag{6.8}$$

where σ and β are to be determined. Substitution in equation (6.3) gives the self-similar form

$$R^{\nu} \cos \nu\theta - \nu^2 R^{2\nu-2} + C = 0 \tag{6.9}$$

provided that the powers of t in (6.3) are all equal, that is

$$\nu\beta - \tfrac{4}{3} = (2\nu - 2)\beta - \tfrac{2}{3} = \sigma. \tag{6.10}$$

These relations are satisfied if

$$\beta = \frac{2}{3(2-\nu)}, \quad \sigma = \frac{2(3\nu-4)}{3(2-\nu)}. \tag{6.11}$$

When ν is close to one, then β is nearly $\frac{2}{3}$ and the acceleration $\ddot{r}$ varies as $t^{-4/3}$ as before. Also $\sigma \simeq -\frac{2}{3}$. A typical sequence of surfaces is shown in figure 13, which may be compared with figure 11.

7. Conclusions

In at least three different physical situations the formation of a critical jet in an axisymmetric cavity has been found to be characterized by a power-law dependence of the velocity and acceleration on the time t. The exponent $(-\alpha)$ in the power law is not a constant, but seems to be related to the angle θ_c of inclination of the local 'asymptotes' to the direction of the axis.

A simple model of the local velocity potential as a spherical harmonic of degree ν leads to the conclusion that when ν is close to one then α should be nearly $\frac{4}{3}$. Moreover as θ_c increases, ν diminishes and α should increase. These expectations are borne out by the numerical calculations.

On the other hand the free surface profiles, though in qualitative agreement with the numerically calculated profiles, do not match them accurately, so that equation (5.1) can be only a first approximation.

An analogous situation exists for steep gravity waves meeting a vertical wall. The strong upwards jet, or 'flip-through' described by Cooker & Peregrine can be interpreted as a critical microjet in two dimensions. Again it is found that the acceleration of a particle at the wall has a power-law dependence on the time. This likewise is explained by a simple analytic model (equation (6.1)), but again a single term does not accurately match the free surface. There is clearly more to be done on this problem.

We are indebted to Dr M. J. Cooker for supplying the numerical values of the acceleration used in §6. The physical example in §4 (bubble collapse near a wall) was suggested by Professor J. R. Blake. This work has been supported by the Office of Naval Research under Contract N00014-91-J-1582 and by the US National Science Foundation under Grant CTS 9318724.

Appendix A. Proof that $(1-\nu)$ divides $\mathrm{d}\Phi/\mathrm{d}\mu$

From the definition of Φ in equation (5.3) we have

$$\Phi' = 2P'_\nu[\nu^2 P_\nu - \mu P'_\nu + (1-\mu^2)P''_\nu]. \tag{A 1}$$

The second derivative P''_ν can be eliminated by using the differential equation for $P_\nu(\mu)$ (Whittaker & Watson 1927, ch. 15) to give

$$\Phi' = 2P'_\nu[\mu P'_\nu - \nu P_\nu]. \tag{A 2}$$

But from the expansion (5.5) we have

$$P_\nu = 1 + \tfrac{1}{2}\nu(\nu+1)(\mu-1) + R, \tag{A 3}$$

where R is divisible by $(\nu-1)$. Substitution from (A 3) into (A 2) gives

$$(\mu P'_\nu - \nu P_\nu) = (\mu R' - \nu R) - \tfrac{1}{2}(\nu-1)[(\nu+1)\mu - (2+\nu)], \tag{A 4}$$

which is divisible by $(\nu-1)$. Hence Φ' also is divisible by $(\nu-1)$.

References

Blanchard, D. C. & Woodcock, A. H. 1980 The production, concentration and vertical distribution of the sea-salt aerosol. *Ann. N.Y. Acad. Sci.* **338**, 330–347.

Cooker, M. J. & Peregrine, D. H. 1990 Water wave impact: computations, theory and a comparison with measurements. In *Proc. 6th Int. Workshop on Water Waves and Floating Bodies*, Woods Hole, MA, USA, pp. 49–53.

Cooker, M. J. & Peregrine, D. H. 1991 Violent surface motion as near-breaking waves meet a wall. In *Breaking waves* (ed. M. L. Banner & R. H. J. Grimshaw) (*Proc. IUTAM Symp., Sydney, Australia*), pp. 291–287. Berlin: Springer.

Longuet-Higgins, M. S. 1983 Bubbles, breaking waves and hyperbolic jets at a free surface. *J. Fluid Mech.* **127**, 103–121.

Longuet-Higgins, M. S. & Oğuz, H. 1995 Critical microjets in collapsing cavities. *J. Fluid Mech.* **290**, 183–201.

Oğuz, H. N. & Prosperetti, A. 1990 Bubble entrainment by the impact of drops on liquid surfaces. *J. Fluid Mech.* **219**, 143–179.

Plesset, M. S. & Chapman, R. B. 1971 Collapse of an initially spherical vapour cavity in the neighbourhood of a solid boundary. *J. Fluid Mech.* **47**, 283.

Whittaker, E. T. & Watson, G. N. 1940 *A course of modern analysis*, IVth edn, p. 608. Cambridge University Press.

PHILOSOPHICAL TRANSACTIONS OF THE ROYAL SOCIETY A MATHEMATICAL, PHYSICAL & ENGINEERING SCIENCES